

# Soft Robotic Actuator Leveraging Switchable Strain-Limiting Structures for Tumor Biopsy and Ablation in MRI

Jan Peters<sup>1</sup>, Johann Licher<sup>1</sup>, Bennet Hensen<sup>2</sup>, Frank Wacker<sup>2</sup>, Annika Raatz<sup>1</sup>

**Abstract**—Despite its multiple advantages over classical procedures, interventional magnetic resonance imaging (iMRI) remains a rarely used method in percutaneous tumor biopsy and ablation of the liver. Mainly due to the difficult and special environment in the MRI scanner, automation of the process through the use of robots remains a challenge. Soft robotic systems, made of soft materials and actuated by pneumatic pressure, offer a way to assist interventionalists in their daily work in iMRI. In this paper, we present a soft robotic actuator that leverages switchable interlocking strain-limiting structures for bending and position locking. Comb-like structures in separate chambers are used to create the actuator’s bending motion through force-transmitting form-closure.

## I. INTRODUCTION

Liver cancer is one of the most common types of cancer worldwide and the incidence of liver cancer is increasing significantly, with the number of new cases estimated to rise by more than 50 % until 2040 [1]. This increase is associated with an increasing number of cirrhotic liver patients, the high rate of new hepatitis C infections in the 1960s, 1970s and 1980s, and increasingly frequent obesity [2]. Magnetic resonance imaging (MRI) offers many advantages not only in the detection of cancer, but especially in its treatment [3]. MRI is superior to computed tomography (CT) and ultrasound in the imaging of soft tissue, which is why it is very suitable for the detection and treatment of liver cancer. In addition, the use of MRI enables the avoidance of the exposure to ionizing radiation that occurs with CT. Despite its immense potential, interventional MRI (iMRI) remains a niche field and is practiced only in specialized centers. Reasons for this are the accessibility but also the difficulties in the workflow and automation of the interventions [4]. The major challenges with robotic automation in iMRI are electromagnetic interference from electrical components, material incompatibilities when using metals, and general confinement within the MRI [5]. Soft robotic systems, especially pneumatically operated ones, offer a unique opportunity here: The materials used for manufacturing are MRI compatible, the actuators do not require any electrical components, and the inherent safety due to their softness helps in the close interaction between interventionalist, patient, and robot.

As described in detail in [6] and shown in Fig. 1, the goal of

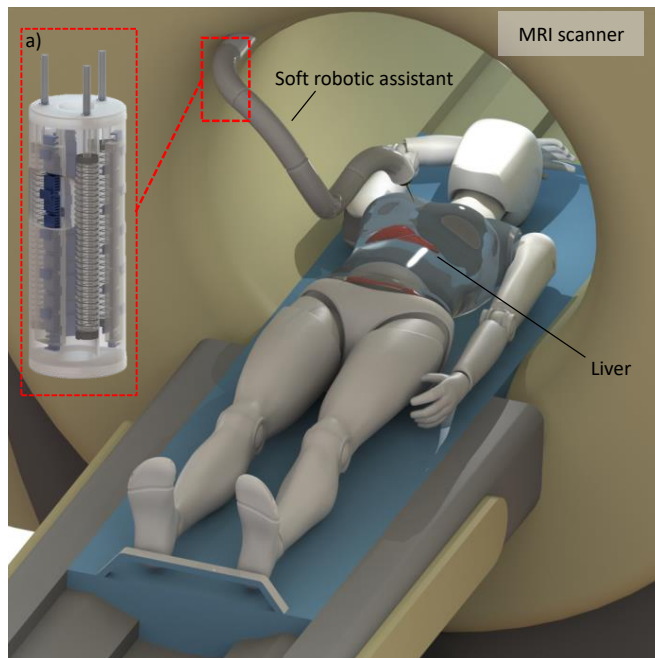


Fig. 1. Concept of the proposed soft robotic assistant for percutaneous tumor biopsy and ablation in magnetic resonance imaging. Several soft pneumatic actuators can be connected modularly to form an assistance system. The actuator with switchable strain-limiting structures is shown in section a).

this project is an automated soft robotic arm that serves as an assistant to the interventionalist by securing the needles used for biopsy (sampling) and ablation (elimination) of the tumors, thus serving as a third arm in the MRI bore. This paper describes the soft actuators used for the automated soft robotic arm in detail.

In soft material robotics, the boundaries between actuators, joints, links and sensors as known from classical robotics are blurring, which means that actuators must be able to do much more than simply generate motion and force. By using soft materials, actuators can also react to their environment through morphological adaptation, actively change their stiffness or, in the case of pneumatic soft actuators, passively vary their stiffness through contact forces. The motion of these actuators is usually pre-programmed into the material through the use of strain-limiting structures [7], [8], [9]. These can be, for example, threads for reinforcement that prevent radial expansion in pressure chambers and translate the energy of the actuation pressure (in the case of pneumatic or hydraulic actuation) into axial elongation. Non-stretchable or two-way stretchable textiles are also commonly used

Funded by the Deutsche Forschungsgemeinschaft (DFG, German Research Foundation) under grant no. 405030609.

<sup>1</sup>Jan Peters, Johann Licher and Annika Raatz are with the Institute of Assembly Technology and Robotics, University of Hannover, Hannover, Germany [peters@match.uni-hannover.de](mailto:peters@match.uni-hannover.de)

<sup>2</sup>Bennet Hensen and Frank Wacker are with the Institute of Diagnostic and Interventional Radiology, Hannover Medical School, Hannover, Germany

in soft robotics to make soft actuators bend, for example. Common to all strain-limiting structures is that they are permanently embedded in the material of the actuator, thus pre-determining the trajectory of the actuator. In this paper, we investigate another possibility of enabling the actuator motion to be controlled by strain-limiting structures that are switchable. This results in fewer actuation sources, such as valves, being required and, ultimately, in fewer, but more versatile, soft pneumatic actuators - a key factor when it comes to the clinical use in a confined operating room. In Section II the concept, design, and fabrication of the proposed soft robotic actuator leveraging switchable strain-limiting structures are explained. Section III gives an overview of the experiments which were performed to validate our concept as well as the used test setup. In the following Section IV the results of the validation are presented and then discussed in Section V. Section VI outlines the conclusions drawn from this work and provides an outlook for future developments.

## II. CONCEPT, DESIGN, AND FABRICATION OF THE SOFT ROBOTIC ACTUATOR

### A. Concept of the Strain-Limiting Structures

There are various ways of enabling strain-limiting structures to be switchable. The necessary force transmission, which limits the strain locally and directionally, can take place in a material-locking [10], [11], force-locking [12] or form-locking manner [13]. By using a low-melting point alloy, we were able to switch strain-limiting structures on and off in a material-locking manner in a previous work [14]. The switching can thus happen through thermal energy in the material itself. Jamming (granular, tensile or layer jamming), which is often used as a stiffness-variable mechanism, can also be used as a switchable strain-limiting structure [12]. Here, force transmission occurs due to the application of negative pressure, i.e., fluidically activated, under force closure. In this paper we investigate the possibility of activating (locking) and deactivating (unlocking) the force transmission by form closure, using only positive pressure to avoid additional equipment needed for negative pressure.

We have developed a mechanism based on 3D-printed comb-like structures that interlock with teeth to create a form-closure force transmitting connection. These comb structures are integrated into the walls of chambers, as shown in Fig. 2. The actuator has six chambers in total: three actuation chambers and three comb chambers. If these comb chambers are pressurized, they expand radially and the combs are pulled apart (unlocked). If the whole actuator then elongates due to pneumatic pressure in the three actuation chambers, the combs can move freely against each other and the elongation (strain) of the actuator is not limited. When the pressure is released, the energy stored in the deformed silicone ensures that the combs are pressed together again (locked), thus restoring a strain-limiting connection between the upper and lower actuator part on one side. If the actuation chambers are pressurized now, the actuator bends over the strain-limited side. To be able to steer the actuator in different directions,

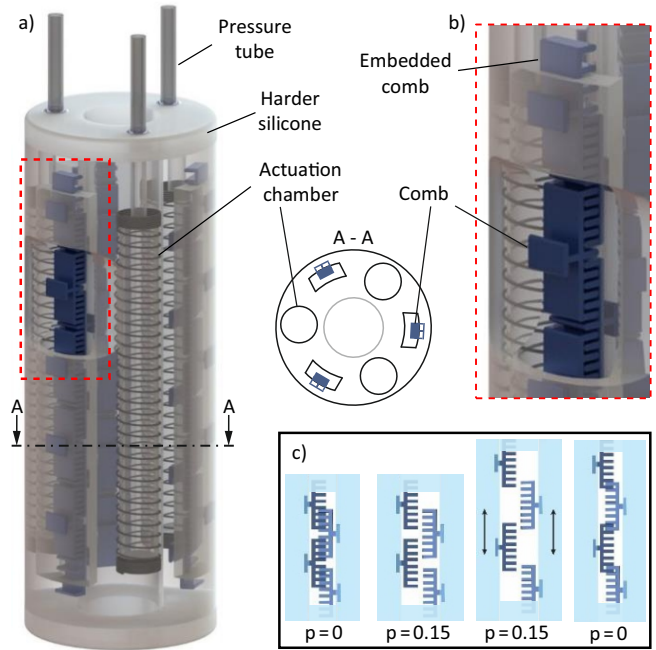


Fig. 2. a) Soft robotic actuator featuring comb chambers for switchable strain-limiting structures. b) Cut out showing the combs. The top comb is embedded into the surrounding silicone to fix it to the top actuator cap. c) Sequential representation (from left to right) of the process of unlocking, elongation, and locking. The corresponding pressures in bar are indicated below.

three comb chambers are integrated into the actuator. If two of the three comb chambers are locked at the same time, the actuator can also bend over the resulting sides. The actuator is thereby able to bend into six directions with only one pressure regulator used for the actual elongation of the three actuation chambers. If all three comb chambers are first pressurized and thus unlocked, the actuator will elongate instead of bend due to the pressure in the actuation chambers. The combs then allow the actuator to be held in its elongated position when pressure is removed from the comb chambers and the combs interlock with each other again.

Unlike approaches based on jamming, this actuator uses positive pressure only - both for actuation and to enable and disable the strain-limiting structures. In comparison to the already presented concept of using a low-melting-point alloy, this approach does not require any metal or electrical components - a requirement for the use in magnetic resonance imaging. The passive (unactuated) state represents the locked and thereby safe configuration, which can be seen as a safety feature in case the pneumatic air pressure supply fails.

### B. Design, Fabrication, and Materials of the Soft Robotic Actuator

As illustrated in Fig. 2, the soft actuator consists of a 95 mm long silicone main body (Ecoflex 00-50, SmoothOn) with three circular shaped actuation chambers (10 mm diameter) that are reinforced with a helical thread to prevent radial

expansion, allowing axial elongation only. The three comb chambers are each positioned circumferentially and centered between the actuation chambers. Each comb chamber has a length of 65 mm and is equipped with six combs, the first and last of which are embedded in the silicone both on the back of the comb and on the respective top or lower side of the comb. The combs in between are only embedded in the silicone by small bars at the back of the comb. To bond the 3D-printed combs with the silicone, the 3D-printed structure is designed to let the silicone flow into slots, similar to the bonding process presented in [15]. The center of the actuator forms the working channel of the whole soft robotic arm.

The manufacturing process consists of five steps: First, the 12 mm diameter cores for the three actuation chambers are wrapped with the polyester thread and are placed in the main body mold. Each actuation chamber core consists of three parts and can thus be disassembled and individually pulled out of the cured silicone body without damaging the wrapped thread. The winding is done thread by thread and thus without leaving any space in between. Additionally, the three comb chambers are assembled inside the main mold. Each of the three comb chambers is molded by three cores: one core for the chamber itself and one core each that contacts the outside and inside of the actuator mold, thus leaving space in the cured silicone for the assembly of the combs. All cores are placed in the main actuator mold, and the silicone main body is cast.

In the second step, the combs are placed in the comb chambers and fixed in the actuator's outer walls. For this, the combs are inserted into the chamber from above and brought into their respective positions. Then, at the height of the bars on the back of the combs, 3 mm wide cuts are made in the silicone to fix the bars in the silicone wall. For the actuation chambers, thinner cores (10 mm diameter) are placed in the actuation chambers to create a silicone skin under the winded thread.

The highest comb is half cast in silicone in a separate mold and then inserted into the top of the comb chamber. In this way, the chambers are closed at the top and the entire mold can be covered with another layer of Ecoflex 00-50 in the next step. Thereby, the exposed sides of the comb chambers are filled, thus fixing the combs in position and sealing the whole actuator at the top with a cap. After the silicone has cured, the inner cores of the actuation chambers can be removed downwards through the pressure tube channels. Two additional casting steps follow, in which a harder silicone layer (DragonSkin 30, SmoothOn) is added to the bottom and top of the actuator to give it more stability. All previously described silicone casting processes included degassing after mixing the two silicone components and curing for minimum 12 hours.

The last step is to glue tubes (silicone tube, 4 mm diameter) into the designated channels. To pressurize the comb chambers, cannulas (1 mm, B. Braun) are inserted into the chambers from below. Tubes are connected to these cannulas via Luer Lock connectors.

The 3D-printed combs used here (PLA, Prusa) have 1 mm

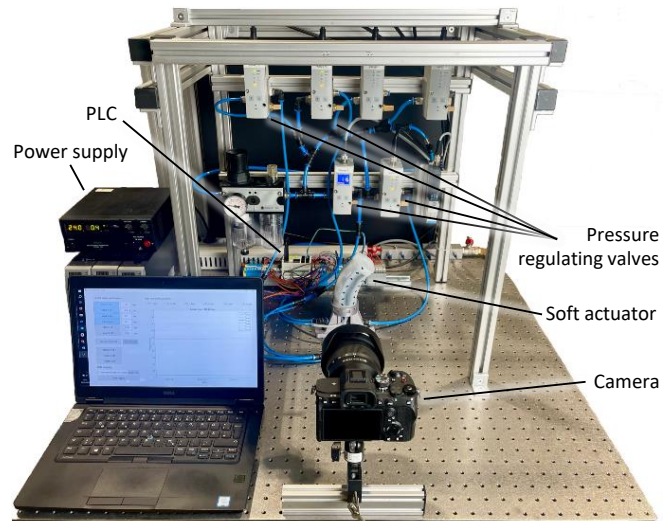


Fig. 3. One proportional pressure regulator is connected to the combined actuation chambers and three additional proportional pressure regulators are used to activate/deactivate (lock/unlock) the three comb chambers. The actuator's motion is tracked by a camera and markers which are applied to the surface of the actuator. The actuator can be seen in its bending configuration.

thick teeth and are 4 mm wide. There is a space of 2 mm between each tooth. This ensures that the combs can tilt against each other to a certain extent, which in turn leads to a certain bendability in the locked state. This is necessary because otherwise the combs would not only prevent elongation on one side but also bending over this side. To ensure that the combs do not separate from each other and reliably interlock, the teeth have 1.2 mm diameter knobs on their ends.

### III. EXPERIMENTS AND TEST SETUP

#### A. Experimental Protocol

Three experiments were conducted to investigate the characteristics of the actuator and the strain-limiting structures. For this purpose, the bending of the actuator at increasing actuation pressure was investigated in Experiment 1, the bending and elongation for different interlocking comb combinations in Experiment 2, and the elongation at increasing pressure and the position-locking capability in Experiment 3. The test setup is shown in Fig. 3. In addition, an experiment on the MRI compatibility of the used materials was performed (Experiment 4):

Experiment 1: To investigate the bending of the actuator, the actuator is pressurized from 0 to 1.1 bar. First, two of the three comb chambers are unlocked (pressurized with 0.15 bar) so that the actuator bends over the remaining third comb chamber when actuated. The test is repeated three times.

Experiment 2: In Experiment 2, five different configurations of the actuator are tested and compared with each other. First, the three comb chambers are compared with each other. For this purpose, comb chambers 2 and 3 are unlocked first and

then the pressure is increased to 1.1 bar in order to measure the bending over comb chamber 1 (the same test as in Experiment 1). Equally, the bending over comb chambers 2 and 3 are measured in the same way. The actuator can also be bent over two combined comb chambers. For this, comb chamber 3 is unlocked while comb chambers 1 and 2 are kept locked. In a last test, all three comb chambers are unlocked and pressure is applied to the actuator, causing it to elongate axially. All tests compare the actuator configuration for 0 and 1.1 bar and are performed three times each.

Experiment 3: A special feature of the comb chambers as strain-limiting structures is the ability to hold the actuator in an extended position (called position locking here). All three comb chambers are first unlocked so that the actuator elongates when pressurized with 0.8 bar. Due to the limited length of the combs, the actuator was only actuated up to 0.8 bar here, since larger elongations could no longer be locked by the combs. The pressure in the three comb chambers is then released so that the combs are locked. Now the actuation pressure is lowered to 0.0 bar and the position is measured. The test is repeated three times.

Experiment 4: To test the MRI compatibility of the materials used, a previous actuator version made of the same materials (Ecoflex 00-50, Dragon Skin 30, 3D-printed PLA, silicone tubes) was tested in an MRI (Siemens MAGNETOM Avanto) using gradient echo measurements and evaluated by the signal-to-noise ratio. In order to make a comparison, measurements are made with a reference fluid and with the actuator and the reference fluid.

### B. Test Setup Used for Experiments

To test the new actuator concept, a test bench consisting of four pressure-regulating valves controlled by a programmable logic controller (Controllino Mega Automation) was set up. Only one proportional pressure regulator (VPPM-6L-L-1-G18-0L2H-V1P-S1C1, FESTO) is connected to all three pneumatic chambers for actuation and three additional pressure regulators (VPPM, Festo) are connected to each of the chambers with the interlocking comb structures to lock/unlock them. The comb chambers are locked/unlocked with a constant pressure of 1.5 mbar but the nearby actuation chambers and the length change create a need for actively regulating the pressure in the comb chambers. A user interface is realized by a MATLAB GUI connected to the programmable logic controller. In addition to the control, the measured pressures can be logged and monitored in a live plot. The actuator's motion is tracked using a video camera (alpha 7, Sony) and black markers on the actuator's surface. Between measurements, the actuator was rotated around its longitudinal axis to achieve perpendicularity of the camera axis and the plane of bending.

## IV. EXPERIMENTAL RESULTS

### A. Experiment 1: Bending over one locked chamber with increasing actuation pressures

The bending of the actuator over one locked comb chamber for different actuation pressures is shown in Fig. 4. Minor bending already occurs when unlocking (pressurizing) the comb chambers (red 0.0 bar curve). Bending increased for every pressure step until the maximum applied pressure of 1.1 bar. The maximum deflection at the actuator tip is 29.2 mm (SD=0.77 mm) in x and 14.0 mm (SD=0.35 mm) in y-direction. Buckles in the curve reflect the measuring method through discontinuous tracking markers and does not directly reflect the bending curve of the actuator backbone.

### B. Experiment 2: Comparison of different actuator configurations

The results of Experiment 2 are shown in Fig. 5. Actuation with 1.1 bar leads to bending with a tip deflection of up to 30.5 mm in x-direction for one locked comb chamber and 21.6 mm for two combined comb chambers in the locked state. The combined elongation (curve length measured using spline interpolation) due to pressurization is higher for bending over one comb chamber (116.6 mm, SD=0.28 mm) compared to bending over two comb chambers (111.0 mm, SD=0.10 mm). Pressurizing (unlocking) all three comb chambers and actuation with 1.1 bar leads to an elongation of 123.3 mm (129%). Minor deviation in x-direction with a maximum of 1.6 mm occurs in the middle of the actuator (compared to the unpressurized reference actuator).

### C. Experiment 3: Elongation and position locking of the actuator

Fig. 6 shows the elongation of the actuator when pressurized to up to 0.8 bar after all three comb chambers have been unlocked (Measurement 1, 0.0 bar). The elongation of the actuator reaches 114.2 mm (SD=0.83 mm). The comb chambers are then locked again and the actuation pressure for the actuator is released. The resulting measurement (Measurement 6) shows a remaining elongation of 105.9 mm (SD=0.98 mm) and a slightly turned tip orientation.

### D. Experiment 4: MRI compatibility

With the help of a gradient echo measurement in the MRI and the analysis of the signal-to-noise ratio (SNR), the components of the soft robot are tested to determine if they cause interference. Fig. 7 gives an example of the cross-sectional images that result from measuring with the reference fluid only and with the reference fluid and the actuator at the same time. The SNR of the reference measurement is 11.32 dB (SD=0.13), which is in the same order of magnitude as the measurement including the actuator (SNR=11.46, SD=0.10). The materials used thus do not lead to a degradation of image quality in the MRI.

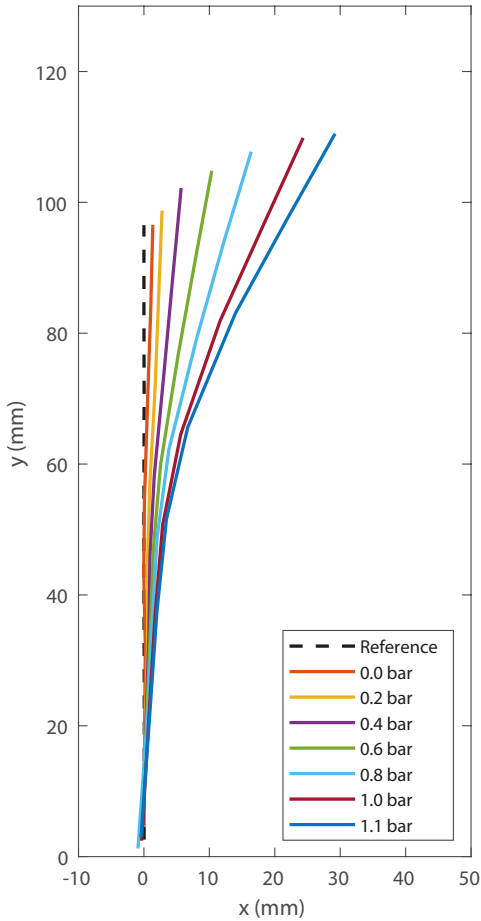


Fig. 4. Actuator bending for pressure steps up to 1.1 bar applied to all actuation chambers while comb chamber 1 is locked and the other two are unlocked. The red curve (0.0 bar) represents the actuator for 0.0 bar actuation pressure but after pressurization of the two comb chambers, which leads to minor bending when compared to the reference (0.0 bar actuation pressure and no pressurized comb chambers).

## V. DISCUSSION

The conducted tests in Experiment 1 show continuous combined bending and elongation for increasing actuation pressures. The elongation results from the tolerances in between the comb teeth and the elongation in the top and bottom cap of the actuator. The comparatively small standard deviation shows the repeatability of this new type of bending via switchable strain-limiting structures.

When comparing the motion for one and two locked comb chambers in Experiment 2, the configuration with two locked comb chambers shows less bending and less elongation. This is, firstly, due to the shorter lever arm formed by the combined comb chambers. The lever arm is shorter because the actuator bends over the point in the center of the two locked comb chambers, which is closer to the center of the actuator. Secondly, one of the three chambers for actuation lies between the two locked comb chambers and thus cannot contribute to the bending of the actuator. At the same time, however, this results in less elongation because two locked comb chambers can prevent axial elongation better than

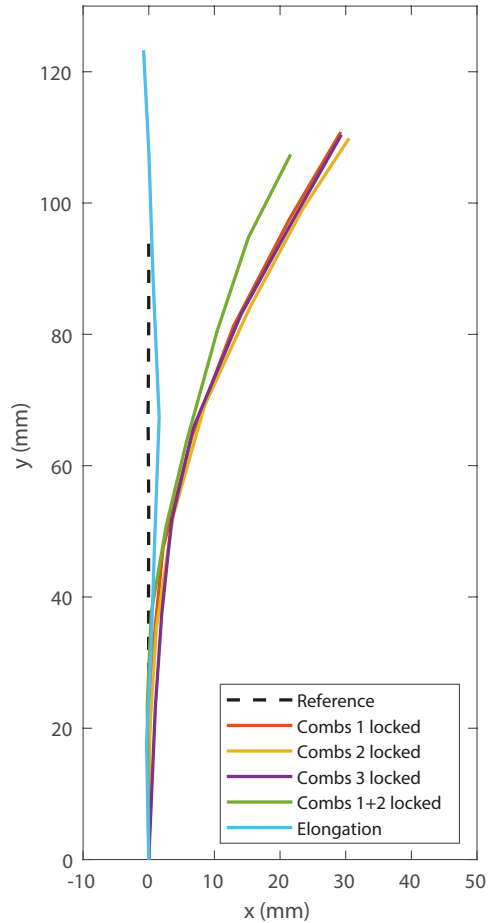


Fig. 5. Bending and elongation of the actuator for a pressure of 1.1 bar. Bending is shown for one locked comb chamber (red, yellow, and purple curve) and for two locked comb chambers (green curve). The actuator was oriented so that bending always occurred perpendicular to the camera axis. The reference line shows the actuator without any (actuation chamber or comb chamber) pressure. Elongation of the actuator (all three comb chambers are unlocked) is represented by the blue curve.

one comb chamber alone. Consequently, having all comb chambers in the unlocked state and thereby no activated strain limiting layers lead to the greatest actuator elongation. In Experiment 3 the elongation for different actuation pressures and the position locked actuator are shown. For measurement 1 no elongation is visible for 0.0 bar, but deviations in x-direction occur due to the comb chambers being pressurized. The actuator does not have reinforcements against expansion in the radial direction in the comb chambers, which leads to mainly radial expansion with limited axial elongation. The radial expansions are very sensitive to manufacturing inaccuracies, ultimately leading to the visible deflections in x-direction.

Elongation in the position-locked state (Fig. 6, Measurement 6) is significantly lower than in the unlocked but pressurized state (Fig. 6, Measurement 5). One reason for this is the used combination of comb teeth distance and the comb thickness which leaves a considerable gap. This is necessary to ensure that the combs still reliably grip each other when elongated and to allow bending of the

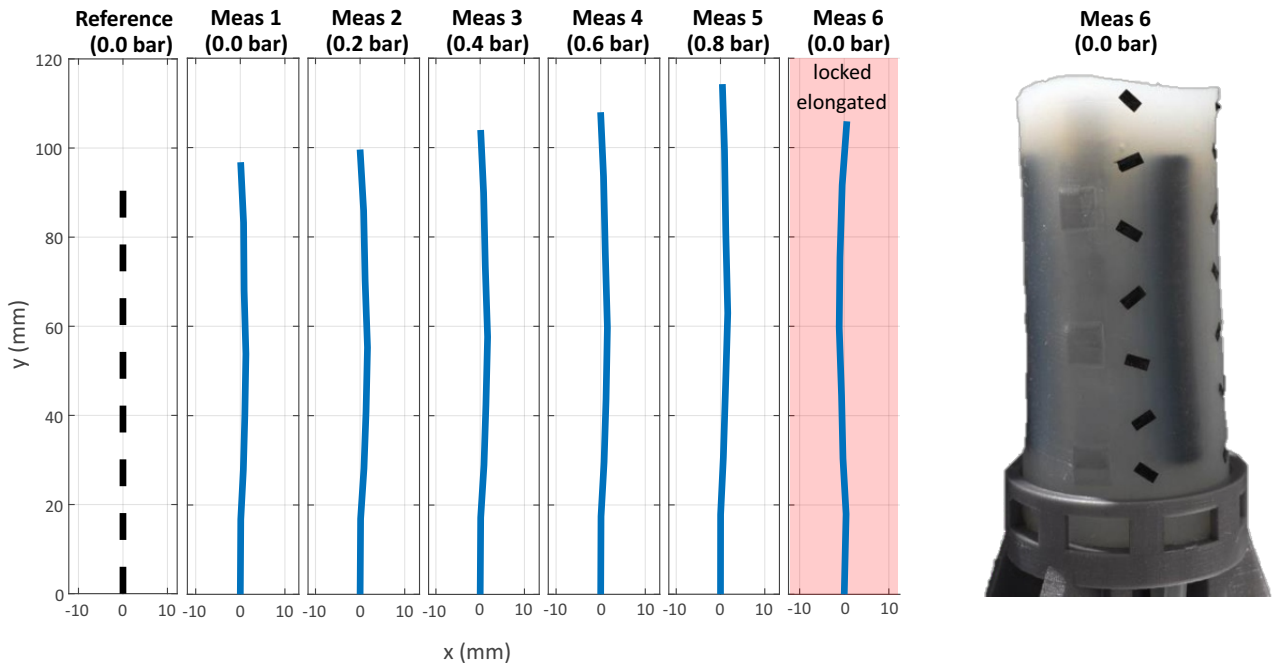


Fig. 6. Actuator configuration for increasing pressures applied to all actuation chambers while all comb chambers are unlocked. The difference between the reference and the 0 bar curve is due to the pressurization of the comb chambers which leads to minor bending. For the locked elongated state, all comb chambers were locked while the actuation pressure was at 0.8 bar and then set to 0 bar.

interlocking combs. When the actuation pressure is removed, however, this subsequently leads to a decrease in elongation. Another factor is the elongation of the end caps of the actuator, which cannot be absorbed by the comb structures and thus contract again when the pressure is removed. This effect is also visible by the uneven shaped top surface of the actuator tip.

While the tip orientation does not change between measurement 1 and 5, the locked actuator changes to a right-leaning tip orientation. This is the result of the combs on one side (here on the right) gripping lower than on the other side when they are brought together. With this type of mechanism, the locking only fits at discrete intervals, which correspond to the distances between the individual teethes of the combs.

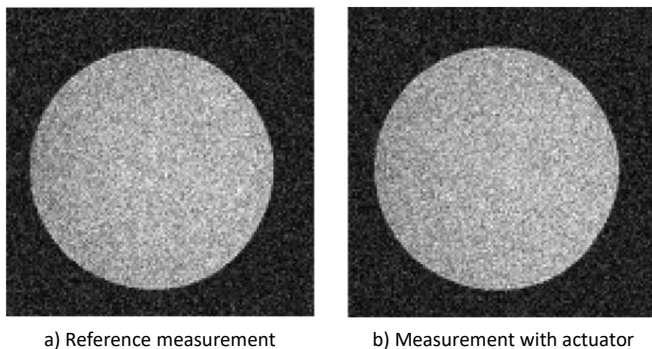


Fig. 7. Cross-sectional images of the gradient echo measurement for comparison of the a) reference fluid and b) the reference fluid with the actuator in addition.

## VI. CONCLUSIONS

In this paper, we presented our new concept and design for a soft robotic actuator leveraging switchable interlocking strain-limiting structures. The actuator is able to steer in six different directions with just one valve being used for actuation. The comb-like structures are used as the strain-limiting parts inside the soft actuator, transforming the actuation pressure into bending or elongation motions depending on their state. In addition, locking the comb chambers while in an actuated state leads to a position lock of the actuator when elongated. Locking was also tested for bent configurations. However, the combs are not able to hold a bent position because of the combs' shape. The straight teeth cannot interlock, when being rotated against each other. The combs slide on each other until the actuator is back in a straight configuration. At this point the combs' teeth are able to grip into each other again.

In future works we will explore different comb-like structures that should also be able to position lock the actuator in bent configurations. Improvements in the manufacturing process will lead to higher actuation pressures, ultimately resulting in increased bending and elongation capabilities. Furthermore, miniaturization of the comb structures would help reduce the actuator's dimensions and open new applications for deployment. Many more challenges remain to be solved on the way to a fully operational soft robotic assistant for iMRI. Future developments will mainly address the precision of the system under load, where strain-limiting structures like the one presented here could play a major role.

## REFERENCES

- [1] Rungay, H., Arnold, M., Ferlay, J., Lesi, O., Cabaasag, C. J., Vignat, J., Laversanne, M., McGlynn, K. A., & Soerjomataram, I., Global burden of primary liver cancer in 2020 and predictions to 2040. *Journal of hepatology*, 77(6), 1598–1606, 2022
- [2] Llovet, J. M., Kelley, R. K., Villanueva, A., Singal, A. G., Pikarsky, E., Roayaie, S., Lencioni, R., Koike, K., Zucman-Rossi, J., & Finn, R. S. (2021). Hepatocellular carcinoma. *Nature reviews. Disease primers*, 7(1), 6, 2021
- [3] Barkhausen J, Kahn T, Krombach GA, Kuhl CK, Lotz J, Maintz D, et al. White Paper: Interventional MRI: Current Status and Potential for Development Considering Economic Perspectives, Part 1:General Application. *Rofo*, 2017
- [4] Kägebein U, Godenschweger F, Armstrong BSR, et al. Percutaneous MR-guided interventions using an optical Moiré Phase tracking system: Initial results. *PLoS One*, 2018.
- [5] Su, H., Kwok, K., Cleary, K., Iordachita, I., Cavusoglu, M., Desai, J. & Fischer, G. State of the Art and Future Opportunities in MRI-Guided Robot-Assisted Surgery and Interventions. *Proceedings Of The IEEE*. 110, 968-992, 2022
- [6] Schlockermann, K., Peters, J., Hensen, B., Löning C., J.J., Wacker, F. & Raatz, A., Soft Robot Assistance for Tumor Biopsy and Ablation in Magnetic Resonance Imaging. In: Tarnita, D., Dumitru, N., Pislă, D., Carbone, G., Geonea, I. (eds) *New Trends in Medical and Service Robotics. MESROB 2023. Mechanisms and Machine Science*, vol 133. Springer, Cham., 2023
- [7] Ke, X., Jang, J., Chai, Z., Yong, H., Zhu, J., Chen, H., Guo, C., Ding, H. & Wu, Z. Stiffness Preprogrammable Soft Bending Pneumatic Actuators for High-Efficient, Conformal Operation. *Soft Robotics*. 9, 613-624, 2022
- [8] P. Polygerinos et al., “Modeling of Soft Fiber-Reinforced Bending Actuators,” in *IEEE Transactions on Robotics*, vol. 31, no. 3, 2015, pp. 778-789.
- [9] D. Ellis, M. Venter and G. Venter, “Soft Pneumatic Actuator with Bimodal Bending Response Using a Single Pressure Source,” *Soft Robotics*, 8, pp. 478-484, 2021
- [10] Firouzeh, A., Salerno, M. & Paik, J. Soft pneumatic actuator with adjustable stiffness layers for Multi-DoF Actuation. *2015 IEEE/RSJ International Conference On Intelligent Robots And Systems (IROS)*. pp. 1117-1124, 2015
- [11] Gunawardane, P., Budiardjo, N., Alici, G., Silva, C. & Chiao, M. Thermoelastic Strain-limiting Layers to Actively-control Soft Actuator Trajectories. *2022 IEEE 5th International Conference On Soft Robotics (RoboSoft)*. pp. 48-53, 2022
- [12] Yang, B., Baines, R., Shah, D., Patiballa, S., Thomas, E., Venkadesan, M. & Rebecca Kramer-Bottiglio Reprogrammable soft actuation and shape-shifting via tensile jamming. *Science Advances*. 7, 2021
- [13] Liu, J., Yin, L., Chandler, J., Chen, X., Valdastrì, P. & Zuo, S. A dual-bending endoscope with shape-lockable hydraulic actuation and water-jet propulsion for gastrointestinal tract screening. *The International Journal Of Medical Robotics And Computer Assisted Surgery*. 17, 2021
- [14] Peters, J., Sourkounis, C.M., Wiese, M., Kwasnitschka, T. & Raatz, A., Single Channel Soft Robotic Actuator Leveraging Switchable Strain-Limiting Structures for Deep-Sea Suction Sampling, *2023 IEEE/RSJ International Conference On Intelligent Robots And Systems (IROS)*, 2023
- [15] L. Rossing, R. B. N. Scharff, B. Chömpff, C. C. L. Wang, and E. L. Doubrovski, “Bonding between silicones and thermoplastics using 3D printed mechanical interlocking,” *Materials & Design*, vol. 186, p. 108254, 2020